

Hydrogen bonding in Schiff bases – NMR, structural and experimental charge density studies†

Anna Makal,^a Wojciech Schilf,^b Bohdan Kamiński,^{b,c} Anna Szady-Chelmieńska,^d Eugeniusz Grech^d and Krzysztof Woźniak^{*a}

Received 13th April 2010, Accepted 10th October 2010

DOI: 10.1039/c0dt00298d

A series of sixteen Schiff bases (derivatives of salicylaldehydes and aryl amines) was studied to reveal the influence of substituents and the length of the linker on the properties of the H-bonding formed. In theory, two groups of compounds, derivatives of 2-(2-hydroxybenzylidenoamine)phenol and 2-hydroxy-*N*-(2-hydroxybenzylideno)benzylamine, can form different types of H-bonds using one or two hydroxyl groups present in the molecules. Two other groups of compounds, derivatives of 4-(2-hydroxybenzylidenoamine)phenol and *N*-(2-hydroxybenzylideno)benzylamine, can form only one type of H-bond. It was confirmed by ¹⁵N and ¹³C NMR experiments, that in all cases only traditional, H-bonded six-membered chelate rings were formed. The positions of the hydrogen atom in the rings depend on the substituent and phase. Generally, the OH H-bond form dominates in solution, with exception of the nitro derivatives, where the NH tautomer is present. In the solid state the tautomeric equilibrium is strongly shifted to the NH form. Only for the 5-Br derivative of one compound was the reverse relationship found. According to the results of experimental charge density investigations, two intramolecular H-bonds in the 5-methoxy derivative of 2-hydroxy-*N*-(2'-hydroxybenzylideno)benzylamine) differ significantly in terms of charge density properties. The intra- and intermolecular H-bonds formed by the deprotonated oxygen atom from 2-OH group are strong, with significant charge density concentration at the bond critical point and a straight, well-defined bond path, whereas the second intramolecular H-bond formed by the oxygen atom from the 2'-OH group is quite weak, with *ca.* five times smaller charge density concentration than in the previous case and a bent bond path. In terms of energy densities, the latter H-bond appears to be a non-bonding interaction, with total energy density being slightly positive. In terms of source contributions to the density at the H-bond critical point from the atoms involved, the intermolecular, linear H-bond is very strong and charge-assisted in the source function classification, the N(1)–H(1N)···O(1) H-bond is medium-strength, while the third H-bond is extremely weak.

Introduction

Schiff bases are usually obtained by condensation of substituted salicylaldehydes with both aliphatic and aromatic amines. They

commonly form very stable six-membered chelate rings with strong hydrogen bonds. The structure and properties of such bonds have been investigated in the solution and solid state using many physicochemical methods, including heteronuclear NMR in both phases, FT-IR spectroscopy, X-ray and neutron diffraction.^{1–32} In the present study, the structures of four groups of compounds are discussed, obtained by condensation of different salicylaldehydes with 2- and 4-hydroxyaniline and benzylamine and 2-hydroxybenzylamine (Scheme 1).

The compounds from groups **A** and **A'** can theoretically form not only conventional single six-membered chelate rings but also more complicated systems (Scheme 2). The two remaining groups of compounds, **B** and **C**, contain only one hydroxyl group in a favored position in a given molecule. Thus, they can form only conventional hydrogen bonds. Another three compounds, which do not form intramolecular hydrogen bonds, were selected as model reference moieties (Scheme 3). Their spectral parameters

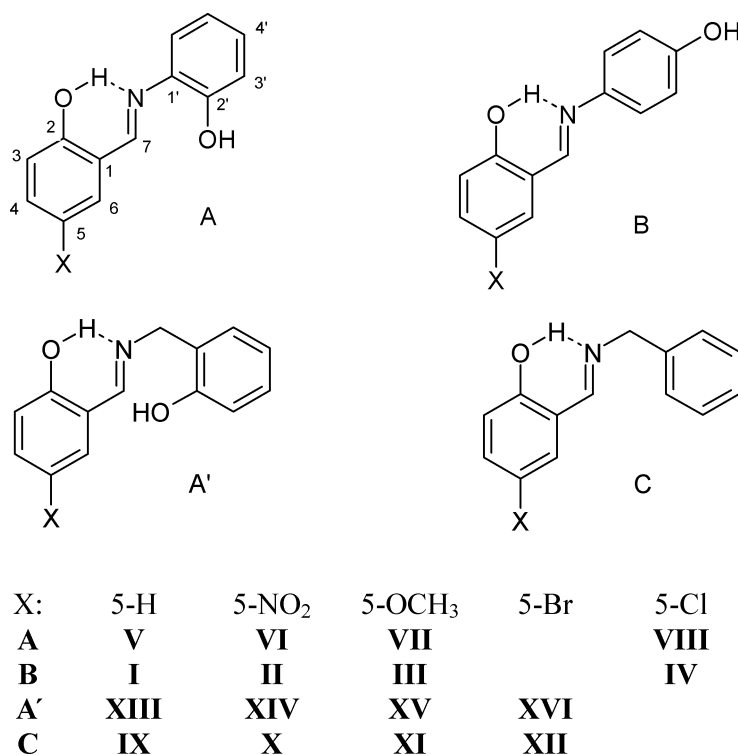
^aDepartment of Chemistry, University of Warsaw, Pasteura 1, 02-093, Warszawa, Poland. E-mail: kwozniak@chem.uw.edu.pl; Fax: +48 22 8222892

^bInstitute of Organic Chemistry, Polish Academy of Science, Kasprzaka 44/52, 01-224, Warszawa, Poland

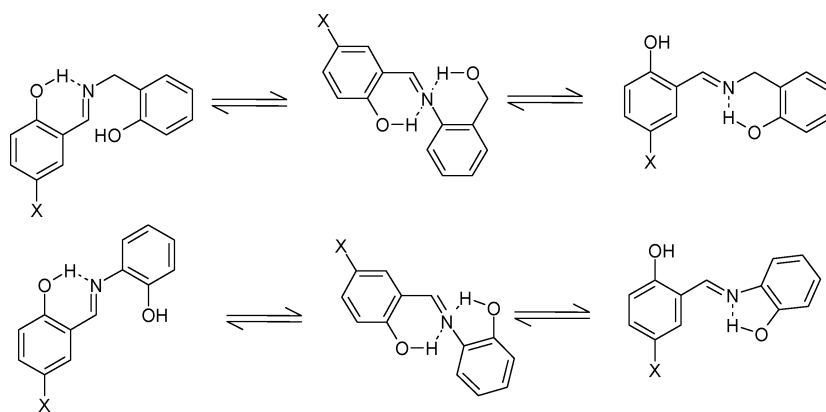
^cInstitute of Physical Chemistry, Polish Academy of Science, Kasprzaka 44/52, 01-224, Warszawa, Poland

^dDepartment of Inorganic and Analytical Chemistry, West Pomeranian University of Technology, al. Piastów 42, 71-065, Szczecin, Poland

† Electronic supplementary information (ESI) available: Technical description of the Experimental section, including details of spectroscopic and crystallographic procedures, crystal data, full table of critical point parameters, residual electron density map, structural and multipole parameters and description of intermolecular interactions. For ESI see DOI: 10.1039/c0dt00298d



Scheme 1 Classes of Schiff bases studied – the X derivatives of: (A) *N*-(5-X-salicylidene)-*o*-hydroxyaniline, (B) *N*-(5-X-salicylidene)-*p*-hydroxyaniline, (A') *N*-(5-X-salicylidene)-*o*-hydroxybenzylamine, (C) *N*-(5-X-salicylidene)benzylamine.



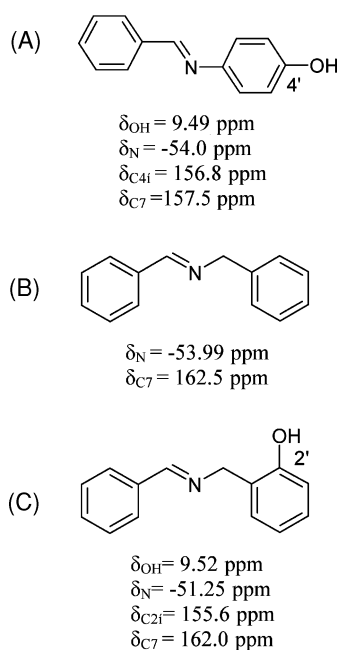
Scheme 2 Possible hydrogen bonding in the studied compounds.

are shown in Scheme 3. The reference compounds from the family **B** contain a short $-\text{CH}=\text{N}-$ linker joining the two aromatic rings, an OH group at the *para* position (unable to form an intramolecular H-bond), and a substituent X (H, NO₂, Ome or Cl).

The compounds from family **C** contain a longer $-\text{CH}=\text{N}-\text{CH}_2-$ linker and they do not have the second OH group. The solid-state structure of compound **I** has already been investigated by X-ray diffraction methods.²⁷ Its asymmetric unit consists of two crystallographically independent, but nearly identical, molecules linked by an $\text{O}-\text{H}\cdots\text{O}$ hydrogen bond. In both molecules typical six-membered hydrogen-bonded rings are found. The two molecules make a dihedral angle of $73.07(4)^\circ$ in the crystal

lattice. They are both roughly planar; however, the benzene ring (C1', ..., C6') in one molecule is slightly more twisted with respect to the (C1, ..., C6, N1, C7) moiety than for the other moiety, as indicated by the values of the dihedral angle between these planes $12.3(1)^\circ$ and $9.7(3)^\circ$, for the first and second molecule, respectively.

The aim of the present study is to find out which schemes of hydrogen bonds are present in the groups **A** and **A'** both in DMSO solution and in the solid state, and characterise these interactions at the level of experimental charge densities. The X-ray structures (Fig. 1) and – in one case – high-resolution charge density studies have been carried out to verify the results of NMR measurements for three compounds **VII**, **XV** and **XVI**.



Scheme 3 Model compounds without hydrogen bonding used as reference systems. All NMR data taken for chloroform solution: (A) *N*-benzylideno-*p*-hydroxyaniline. (B) *N*-benzylideno-benzylamine. (C) *N*-benzylideno-*o*-hydroxybenzylamine.

Results and discussion

NMR

The results of NMR measurements (chemical shifts) are collected in Table 1. From previous experience, we know that the hydrogen atom position in an intramolecular hydrogen bridge can be determined by analysis of the nitrogen chemical shifts of the imine atom (quantitative estimation) or carbon chemical shifts of the carbon atoms bonded to the formal hydroxyl group (qualitative estimation). The general rule is that a transfer of the hydrogen atom from the oxygen atom to the nitrogen atom generates a significant upfield shift of the imine nitrogen signal and a simultaneous downfield shift of the signal of the C–OH atom. The chemical shifts of the remaining carbon atoms in the molecule usually do not supply reliable structural information. This is due to an overlap of several effects influencing this parameter. These are mostly the effects created by different substituents in the aromatic ring. Usually, these effects are very difficult to estimate in three-substituted aromatic rings. Such effects can have similar consequences as those created by different proton positions in the H-bridge.

The proton chemical shift of the OH group can only inform us about the presence of hydrogen bonding (a large downfield effect for the hydrogen-bonded structure) but cannot be used to decide where the proton is located in the H-bridge. Generally, signals from protons located in the middle of the bridge (symmetrical H-bonds) have very large downfield shift compared to signals from the unsymmetrical structures. The following compounds can be used as model reference structures without hydrogen bonding (see Scheme 3): (A) *N*-benzylideno-*p*-hydroxyaniline, (B) *N*-benzylideno-benzylamine, and (C) *N*-benzylideno-*o*-hydroxybenzylamine.

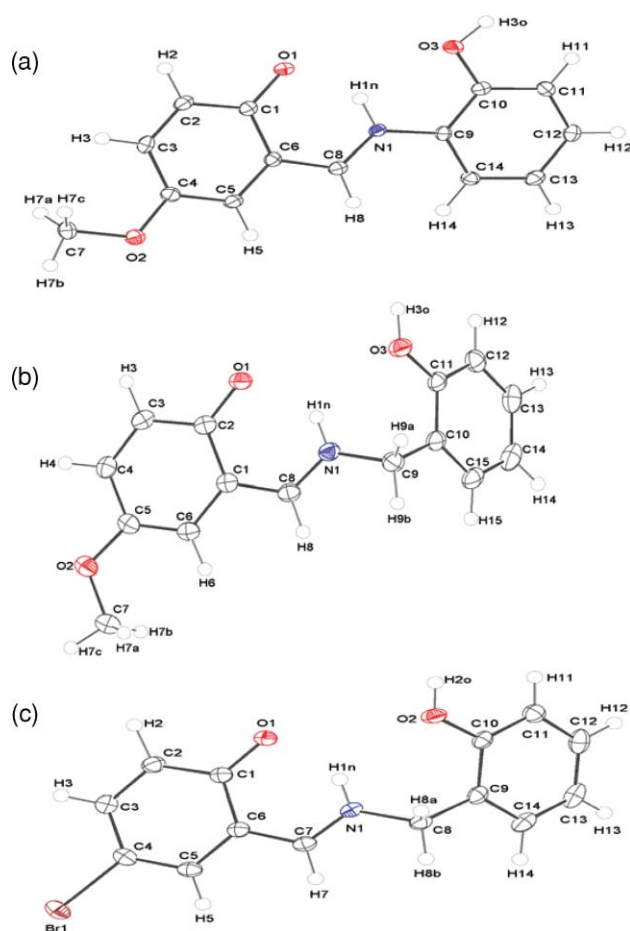


Fig. 1 ORTEP representations of the following compounds: (a) **VII**, (b) **XV** and (c) **XVI**. Thermal displacement ellipsoids are presented at the 50% probability level at 100 K. The most important bond lengths for compound **VII**, **XV** and **XVI** (distances in Å) are listed below: **VII**. O(1)–C(1) 1.310(2); O(3)–C(10) 1.348(2); O(3)–H(3O) 0.93(2); N(1)–C(8) 1.300(2); N(1)–C(9) 1.411(2); N(1)–H(1N) 0.92(2); C(1)–C(2) 1.407(2); C(1)–C(6) 1.432(2); C(2)–C(3) 1.377(2); C(3)–C(4) 1.403(2); C(4)–C(5) 1.376(2); C(5)–C(6) 1.410(2); C(6)–C(8) 1.423(2); C(9)–C(14) 1.391(2); C(9)–C(10) 1.404(2); C(10)–C(11) 1.393(2); C(11)–C(12) 1.387(2); C(12)–C(13) 1.388(2); C(13)–C(14) 1.384(2); **XV**. O(1)–C(2) 1.2979(3); O(2)–C(5) 1.3649(3); O(2)–C(7) 1.4213(4); O(3)–C(11) 1.3440(3); O(3)–H(3O) 0.8823(3); N(1)–C(8) 1.3025(3); N(1)–C(9) 1.4631(3); N(1)–H(1N) 0.8784(2); C(1)–C(2) 1.4284(3); C(1)–C(6) 1.4204(3); C(1)–C(8) 1.4190(3); C(2)–C(3) 1.4264(3); C(3)–C(4) 1.3759(3); C(4)–C(5) 1.4129(3); C(5)–C(6) 1.3751(3); C(9)–C(10) 1.5057(3); C(10)–C(11) 1.4057(3); C(10)–C(15) 1.3940(3); C(11)–C(12) 1.3987(3); C(12)–C(13) 1.3911(3); C(13)–C(14) 1.3940(4); C(14)–C(15) 1.3980(4); **XVI**. Br(1)–C(4) 1.901(2); O(1)–C(1) 1.289(2); O(2)–C(10) 1.355(2); O(2)–H(2O) 0.86(3); N(1)–C(7) 1.284(3); N(1)–C(8) 1.470(2); N(1)–H(1 N) 0.81(2); C(1)–C(2) 1.420(3); C(1)–C(6) 1.439(2); C(2)–C(3) 1.373(3); C(3)–C(4) 1.407(3); C(4)–C(5) 1.365(3); C(5)–C(6) 1.407(3); C(6)–C(7) 1.422(3); C(8)–C(9) 1.502(3); C(9)–C(14) 1.389(3); C(9)–C(10) 1.401(3); C(10)–C(11) 1.391(3); C(11)–C(12) 1.388(3); C(12)–C(13) 1.386(3); C(13)–C(14) 1.390(3).

The third model compound can theoretically form intramolecular hydrogen bonds using the OH group at the position 2', but examination of the nitrogen chemical shift of the imine atom shows that this does not take place. The δ_{N} value of -51.25 ppm is typical for an imine without hydrogen bonding. This means that

Table 1 Proton, carbon and nitrogen chemical shifts of investigated compounds. For the definition of compounds, see Scheme 1.

Compound	Linker	OH, X	DMSO solution				CPMAS									
			δ_{OH}	$\delta_{2\text{OH}}$	δ_{rOH}	δ_{N}	δ_{C2}	$\delta_{\text{C2'}}$	$\delta_{\text{C4'}}$	δ_{C7}	δ_{N}	δ_{C2}	$\delta_{\text{C2'}}$	$\delta_{\text{C4'}}$	δ_{C7}	
I ^b	–CH=N–	4', H	13.4		9.6	-87.1	160.6		157.4	160.6	-99.1,^a -133.8	161.0, 163.1		156.0	159.3, 156.0	
II	–CH=N–	4', NO ₂	15.0		9.8	-99.9	168.2		158.2	158.9						
III	–CH=N–	4', OCH ₃	12.7		9.62	-84.4	154.6		157.5	160.3	-188.4	167.8		157.8	155.4	
IV ^d	–CH=N–	4', Cl	13.5		8.64	-84.9	159.7		157.3	159.2	-166.3	167.4		157.4 ov.	157.4 ov	
V	–CH=N–	2', H	13.7	9.7		-94.6	161.2	151.6		162.1	-215.5	175.7	150.0		153.8	
VI	–CH=N–	2', NO ₂	15.7	10.3		-145.1	173.0	150.9		159.7	-213.9	178.9	149.4		156.4	
VII ^e	–CH=N–	2', OCH ₃	13.0	9.6		-91.3	155.1	151.7		161.9	-200.4	167.8	150.8		154.4	
VIII ^f	–CH=N–	2', Cl	12.2	5.8		-97.2	159.1	147.7		162.4	-192.3	174.2	148.6		160.2	
IX	–CH=N–CH ₂ –	–, H	13.4			-84.1	161.0			166.9						
X	–CH=N–CH ₂ –	–, NO ₂	14.5			-161.3	175.8			167.3	-214.4	179.7			166.2	
XI	–CH=N–CH ₂ –	–, OCH ₃	12.8			-80.3	154.8			166.3	-84.84	154.7			165.0	
XII	–CH=N–CH ₂ –	–, Br	13.5			-82.8	160.5			165.7	-76.3	159.2			163.7	
XIII	–CH=N–CH ₂ –	2', H	13.7	9.6		-87.6	161.4	155.7		166.6	-203.4	174.3	156.8		165.7	
XIV	–CH=N–CH ₂ –	2', NO ₂	15.5	10.0		-182.5	178.0	156.1		167.3	-198.4	179.6	156.8		164.4	
XV ^e	–CH=N–CH ₂ –	2', OCH ₃	13.0	9.58		-82.5	154.9	155.7		165.8	-216.7	170.7	159.8		163.0	
XVI ^e	–CH=N–CH ₂ –	2', Br	13.8	9.6		-89.1	161.2	155.7		165.3	-199.0	173.6	156.6		164.2	

^a Intensity of signals close to 1:1; ov: overlapped signals; –CH=N–: Schiff bases obtained from the aniline derivatives; –CH=N–CH₂–: Schiff bases obtained from benzylamines. ^b X-ray from literature. ^c X-ray from current study. ^d NMR in acetone. ^e NMR in CDCl₃. ^f 5'-CH₃.

the acidity of the OH group at the position 2' is not high enough to form such a bond. Similar conclusion can be obtained when one analyses the OH group proton chemical shifts. This chemical shift is typical for phenols without intramolecular hydrogen bond similarly to the first model compound. Comparing the nitrogen chemical shifts for all model compounds mentioned above, one can say that a typical value for this parameter for a free imine – *i.e.* without hydrogen bonding – is close to –50 ppm.

The structural analysis of the investigated compounds was started using derivatives **I–IV**. The proton chemical shifts of the OH groups (from 12 to 15 ppm) and the nitrogen chemical shifts close to –90 ppm show that in all these compounds intramolecular hydrogen bonding exists. In the CPMAS experiments for **I**, two sets of signals in ¹³C and ¹⁵N spectra were found. This means that the mixture of two different forms of **I** exists in this phase, which is in agreement with the X-ray data. On the base of the δ_{N} values in the DMSO solution, one can determine that the proton transfer process is the most advanced (with the largest upfield shift of the imine signal) in the nitro derivative. In the solid state, this process is even more advanced. For the 5-methoxy derivative, the upfield shift of δ_{N} between the solution and solid state is almost 100 ppm. This is rather an unexpected effect, since for the aliphatic derivative **XI**, the proton position in the bridge (and consequently the nitrogen chemical shifts) are almost the same in the both phases. Similarly, 5-bromo aliphatic derivative **XII** exhibits weaker reaction on transfer from the solution to the solid state (about 10 ppm upfield effect) *vs.* an effect of about 80 ppm compound **IV**.

The second group of compounds, **V–VIII**, is even more interesting because they can form more complicated hydrogen-bond networks (Scheme 2). In this case, on the basis of proton chemical shifts of the OH groups and the nitrogen chemical shifts, one can assume that some intramolecular hydrogen bonds are present. The proton chemical shift values suggest that only the OH groups at the position 2 are involved in this process. The $\delta_{2\text{OH}}$ values are in a typical range for a free hydroxyl group. From nitrogen NMR

data it is evident that in the 5-nitro derivative the proton transfer process is the most advanced ($\delta_{\text{N}} = -145.1$ ppm *vs.* about –90 ppm for the other compounds from this group). The carbon chemical shift of the C2 atom confirms this conclusion. This parameter is different for each compound from this group and generally fulfils the condition that the upfield shift of nitrogen signal of imine is connected with a downfield shift of the carbon atom connected with the OH group involved in the H-bond formation. The value of $\delta_{\text{C2}} = 173.0$ ppm for **VI** is clearly different from the equivalent values for the other compounds, confirming that the C2 atom is involved in hydrogen-bond formation. In contrast to this, the $\delta_{\text{C2'}}$ values for **V–VII** are almost the same. This means that the OH group at this atom does not form H-bonds. The proton and carbon chemical shifts of **VIII** have values that are slightly different compared with **V–VII**. This is probably because of the different solvent used for **VII** (chloroform instead of DMSO) and because of the presence of the methyl group at the aniline ring. This can affect the carbon chemical shifts of the atoms from this ring. In the solid state, **V–VIII** exist in the NH form with almost the same proton position (nitrogen chemical shift very close to –200 ppm in all cases). The $\delta_{\text{C2'}}$ values in the solid state are also very close one to another and to the values found in solution. This means that also in the solid state, the H-bonds in the N···H form exist only at the 2-OH group. If the OH group from position 2' participates in H-bond formation with proton transfer, a downfield shift of the C2' signal should be expected.

The third group of compounds, **IX–XII**, can form only one kind of H-bond because they do not have a second hydroxyl group at a suitable 2' position. One can state – on the basis of nitrogen chemical shifts of the imine atoms – that in the case of the compound **IX**, **XI** and **XII**, some very similar hydrogen bonds with hydrogen atoms located close to the oxygen atom do exist. The 5-nitro derivative, as in the previous groups of compounds, forms a different kind of H-bond in DMSO solution. In this case the bridged hydrogen atom is shifted to the nitrogen site. The analysis of C2 chemical shifts leads to the

same conclusion. In the solid state only three compounds were investigated and similar effects were found. The nitro compound in the solid state exists as the NH form, while the 5-MeO and 5-Br derivatives retain the OH form, resulting in relatively weak hydrogen bonds.

The most interesting is the fourth group of compounds: **XIII** to **XVI**. In this case two different six-membered chelate rings with intramolecular H-bonds can exist (Scheme 2, the upper trace). On the basis of nitrogen chemical shifts analysis (solution NMR spectra) one can say that the compounds **XIII**, **XV** and **XVI** exist as the OH form with some asymmetric intramolecular hydrogen bonding, while the 5-nitro compound exists as the hydrogen bonded NH form. From the nitrogen chemical shifts it cannot be decided which OH group participates in this hydrogen-bond formation. To solve this problem it is necessary to analyze carbon chemical shifts of C2 and C2' atoms. The δ_{C2} values are in good agreement with those in the previously discussed systems, meaning: the upfield shift of the nitrogen signal is connected with the downfield shift of the C2 signal. In contrast to this, $\delta_{C2'}$ values are practically unchanged for all studied compounds and are very close to the $\delta_{C2'}$ value measured for the third model compound ($\delta_{C2'} = 155.6$ ppm) which does not form any intramolecular hydrogen bonding. A comparison of those two effects leads to the conclusion that only the OH groups at the position 2 are involved in hydrogen bond formation with proton transfer, otherwise some downfield effect on $\delta_{C2'}$ would be observed. In the solid state all compounds **XIII–XVI** exist in the NH form, with only very small differences at the hydrogen atom positions. The downfield shift of the C2 signals confirms this statement.

The case of the 5-OMe derivative **XV** in the solid state is a little surprising, as the largest upfield shift of nitrogen signal observed in this study is not accompanied by an equally large downfield shift of the C2 signal. Nevertheless, the carbon signal is still in a range indicating proton transfer from the 2-OH group to nitrogen. This could be explained by intermolecular hydrogen bonding formation in the solid state. This explanation can be verified by analysis of the X-ray data. In general, there are mainly isotropic interactions with the solvent molecules in the solution. This is the reason why the shielding of protons is larger in the solution than in the solid state, whereas in the solid state, there are some strong anisotropic intermolecular interactions with the closest molecules in the crystal lattice.

The crystal structures of VII, XV and XVI

All analyzed Schiff base derivatives crystallize in centrosymmetric space groups (Table 1S†) in the monoclinic system. In each case one molecule occupies a general position in crystallographic asymmetric unit. The ORTEP representations of the compounds at 100 K, together with numbering scheme, are presented in Fig. 1. The symmetry of the crystals does not depend on the temperature, and the general structural motifs, in particular the geometry of hydrogen bonds network, are similar at room temperature and at 100 K. More detailed structural analysis is therefore based on the low temperature datasets, whereas parameters for both temperatures are reported in Table 1S and in deposited cif files. In all compounds investigated by X-ray diffraction an intramolecular asymmetric hydrogen bond is formed, in which the H atom from the C2 hydroxyl group is transferred to the N1 imine nitrogen atom. There are no indications of the alternative proton locations, either at 100 K or at room temperature.

The molecule of **VII** is generally flat. The imine linker of two phenyl rings has a flat geometry and is coplanar with the C1–C6 ring, while the *ortho*-hydroxy-substituted C9–C14 ring is rotated with respect to the Schiff-base plane by about 16° (see Table 4S†). The methoxy substituent is rotated slightly away from the C1–C6 ring by about 6°. Bonds to C1 carbon, connected to strong H-bond donor O1 atom, are elongated by 0.3 Å with respect to the analogous bonds in the rest of the ring, while the OMe substitution does not introduce a similar bias. The C1–C6 ring – as a whole – presents significant bond alternation. The C9–C14 ring, in contrast, has nearly equal C–C distances. Illustration of H-bonded dimers formed in the crystal structures of **VII** at 100 K, **XV** and **XVI** is shown in Fig. 2, the packing and the H-bond networks are shown in Fig. 2S, whereas the details of H-bonds are given in Table 2.

Compounds **XV** and **XVI** represent the A' family of Schiff-base derivatives. An additional methylene group divides the Schiff base fragment from the phenyl substituent, and introduces a bend into the molecules of **XV** and **XVI**. A measure of this bend may be the value of torsion around the N1–C9 bond (**XV**) or N1–C8 bond (**XVI**), reported in the ESI. In the case of the bromine-substituted compound **XVI**, the rotation around the N1–C8 bond is 10° larger than the analogous rotation in **XV**. In both cases, the imine fragment is strictly coplanar with the C1–C6 ring.

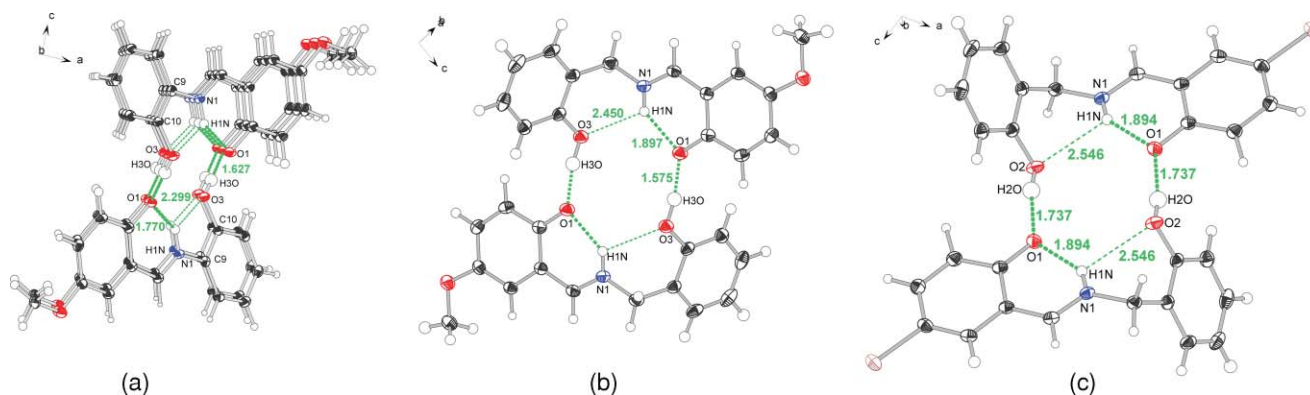


Fig. 2 Illustration of H-bonded dimers in the crystal structures of: (a) **VII** at 100 K, (b) **XV** and (c) **XVI**.

Table 2 H-bond geometries for compounds **VII**, **XV** and **XVI** (distances in Å, angles in °)

D–H···A	<i>d</i> (D–H)	<i>d</i> (H···A)	<i>d</i> (D···A)	∠(DHA)
VII				
N(1)–H(1 N)···O(1)	0.92(2)	1.77(2)	2.551(1)	140(2)
N(1)–H(1 N)···O(3)	0.92(2)	2.30(2)	2.665(1)	102(1)
O(3)–H(3O)···O(1)#1	0.93(2)	1.63(2)	2.558(1)	179(2)
XV at 100 K				
N(1)–H(1 N)···O(1)	0.87(2)	1.90(2)	2.599(1)	137(1)
N(1)–H(1 N)···O(3)	0.87(2)	2.45(2)	2.886(1)	112(1)
O(3)–H(3O)···O(1)#2	0.97(2)	1.57(2)	2.532(1)	170(2)
XVI at 100 K				
N(1)–H(1 N)···O(1)	0.81(2)	1.89(2)	2.589(2)	143(2)
N(1)–H(1 N)···O(2)	0.81(2)	2.55(3)	2.927(2)	110(2)
O(2)–H(2O)···O(1)#2	0.86(3)	1.74(3)	2.582(2)	168(3)

#1: $-x + 1, y - 1/2, -z + 5/2$; #2: $-x + 1, -y + 2, -z$.

Significant bond alternation is present in the C1–C6 ring of **XV**. Elongation of the bonds connected to the oxygen-substituted carbon is also noticeable. The methoxy substituent is out of the C1–C6 ring plane by about 5°. In the case of **XVI**, the C1–C6 ring does not show strict bond alternation, although elongation of the C1-connected bonds is visible. Differences in bond lengths are less pronounced at room temperature.

A common packing motif can be observed for all compounds. For details of the H-bond networks for **VII**, **XV** and **XVI** classified according to the Etter terminology³³ see the ESI.

Hydrogen bonding in **VII**, **XV** and **XVI**

A similar behaviour of the compounds from A and A' group in terms of chemical shifts for atoms potentially involved in hydrogen bonding is in agreement with the structural analysis. Compounds **VII**, **XV** and **XVI** present a common structural motif, which is a specific set of intramolecular hydrogen bonds. In terms of Etter classification, this implies a S21(9) motif for **VII**, and S21(10) for **XV** and **XVI**. Apart from additional methylene group in the compounds of A' series, the motif is the same, consisting of one proton donor – the N1 nitrogen – and two proton acceptors – the oxygen atoms O1 and O3 or O1 and O2 for **XV** and **XVI**, respectively – resulting in the formation of at least one six-membered ring. While the intramolecular N1–H1O···O1 presents in each case features of the typical strong hydrogen bond (Fig. 3), the existence of the actual N1–H1O···O3 (or O2) hydrogen bond may be disputable, due to long donor–acceptor distance and nearly straight D–H···A angle. However, several structural features of the compounds presented here suggest that the interaction takes place. These are: the C–N–C angle values are significantly larger than 120°, indicating the bending of the structure to place the second hydroxyl group closer to the hydrogen donor; the geometry around the O3 or O2 atom, suggesting that the oxygen is bent still closer to the NH group; and the values of angles H–N–C, which are similar, suggesting that the hydrogen is not pulled strongly towards one of the oxygens, but rather is located in between them. Comparison of the most important geometrical features of the intramolecular hydrogen bond motif is presented in Fig. 3.

The formation of this double hydrogen bond is the main cause of the preference for proton transfer from the hydroxyl group on the nitrogen, taking place irrespective of the substituents in

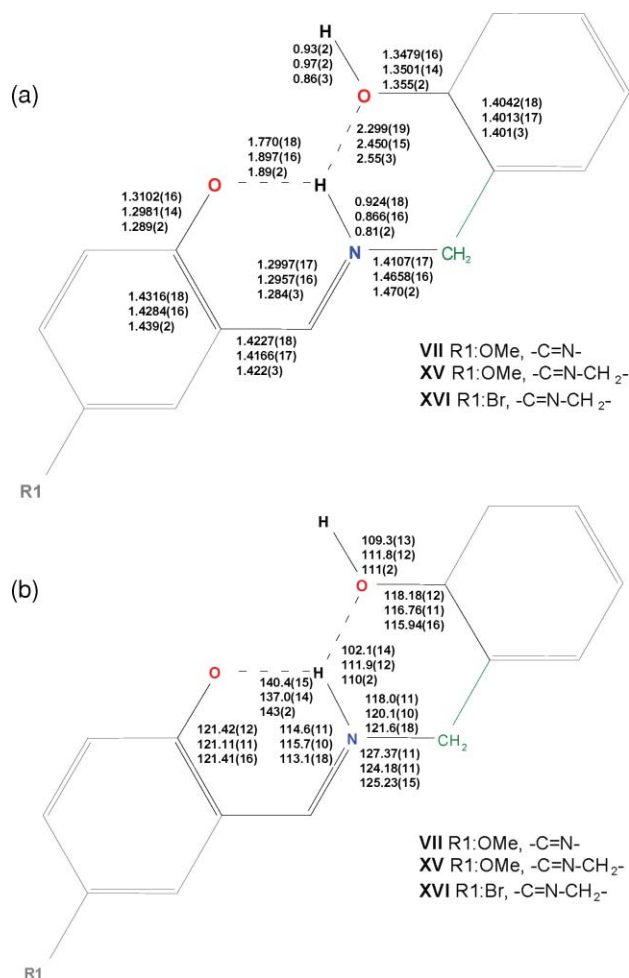


Fig. 3 Representation of the intramolecular hydrogen-bonding system in compounds **VII**, **XV** and **XVI** with selected values of (a) bond lengths and (b) valence angles.

the solid state. While located on the oxygen atom, the proton cannot participate in an additional hydrogen bond with the second hydroxyl group. It is also noteworthy that the hydroxyl group playing the role of hydrogen H1N acceptor, is at the same time an effective donor in intermolecular hydrogen bonds, which are important for the crystal structure stabilization, while they do not exist in the solution.

Experimental charge density analysis of **XV**

Topological analysis of the final model of experimental charge density for **XV** complex was performed. Bond critical points and bond paths have been associated with all covalent bonds and expected hydrogen bonds, both intramolecular and intermolecular. In particular, bond path and bond critical point indicate an additional intramolecular N(1)–H(1N)···O(3) hydrogen bond between the protonated nitrogen atom and the oxygen from 2'-OH group. This hydrogen bond could not be detected by means of NMR study.

A number of intermolecular short contacts can also be associated with BCP-s and bond path existence, reflecting the weak C–H···O interactions of the methoxymethyl group with

Table 3 Most important parameters of experimental charge density at bond critical points in compound XV. Symmetry operation X3: $1 - x, 2 - y, -z$

Bond	$\rho(r_{\text{BCP}})$ [$e \text{ \AA}^{-3}$]	$\nabla^2(r_{\text{BCP}})$ [$e \text{ \AA}^{-5}$]	$G(r_{\text{BCP}})$ [H a_0^{-3}]	$V(r_{\text{BCP}})$ [H a_0^{-3}]	$H(r_{\text{BCP}})$ [H a_0^{-3}]	$G(r_{\text{BCP}})/\rho(r_{\text{BCP}})$ [H e^{-1}]	$H(r_{\text{BCP}})/\rho(r_{\text{BCP}})$ [H e^{-1}]	$ V(r_{\text{BCP}}) /G(r_{\text{BCP}})$
O(1)···H(1N)	0.26(1)	3.33(1)	0.036	-0.037	-0.001	0.92	-0.03	1.03
H(3O)···O(1)_X3	0.47(4)	2.33(7)	0.05	-0.075	-0.025	0.72	-0.36	1.50
O(3)···H(1N)	0.066(5)	1.34(2)	0.011	-0.007	0.003	1.13	0.31	0.64
O(1)–C(2)	2.60(2)	-27.15(8)	0.396	-1.075	-0.678	1.03	-1.76	2.71
O(2)–C(5)	2.21(1)	-18.71(6)	0.318	-0.83	-0.512	0.97	-1.56	2.61
O(2)–C(7)	1.89(2)	-14.59(6)	0.244	-0.639	-0.395	0.87	-1.41	2.62
O(3)–C(11)	2.29(1)	-21.38(7)	0.325	-0.871	-0.547	0.96	-1.62	2.68
O(3)–H(3O)	2.59(1)	-48.55(1)	0.246	-0.995	-0.749	0.64	-1.95	4.04
N(1)–H(1N)	2.82(5)	-38.6(4)	0.402	-1.205	-0.802	0.96	-1.92	3.00
N(1)–C(8)	2.69(2)	-28.87(7)	0.419	-1.138	-0.719	1.05	-1.81	2.72
N(1)–C(9)	1.81(1)	-11.35(5)	0.24	-0.598	-0.358	0.90	-1.34	2.49

O(1) and O(3) atoms from the symmetry-related molecules and C–H··· π interactions. The summary of topological properties for the most interesting interactions is presented in Table 3 (Table 2S† contains full topological data for all bonds). Most of the topological parameters of electron density is close to the values obtained for similar compounds.³⁴

The intramolecular hydrogen bonds differ significantly in terms of charge density properties. The O(1)···H(1N)–N(1) bond is strong, with significant charge density concentration at the bond critical point and a straight, well-defined bond path. The same is true in the case of intermolecular O(1)···H(3O)–O(3) bond. In contrast, the second intramolecular hydrogen bond is weak, showing charge density concentration over five times less than the other H-bonds and a bent bond path, in agreement with the strained geometry. Nevertheless, the topology of the charge density suggests its existence. Moreover, ring critical points of significant charge density concentrations have been found not only for the benzene rings, but also for the six-membered rings associated with O(1)···H(1N)–N(1) and O(3)···H(1N)–N(1) hydrogen bond formation, which according to Koch and Popelier³⁵ criteria makes the topology of the molecule reliable and confirms hydrogen bonding effects (a list of ring critical points reported in the ESI†). In terms of energy densities, the weak O(3)···H(1N)–N(1) hydrogen bond appears as a non-bonding interaction, with the total energy density being slightly positive. It can be qualified as pure closed-shell interaction. This is in line with recent results of Wood *et al.*,³⁶ who concluded that H-bonds with DH···A angles of less than about 130° have negligibly small energies. The NH···O angle of the weak H-bond in XV is 111.9°, so both the geometry, as well as the charge density, points to the weakness of this bond.

The strong hydrogen bonds both qualify as shared-shell interactions with respect to $H(r_{\text{BCP}})$ and $G(r_{\text{BCP}})/\rho(r_{\text{BCP}})$ criteria.³⁷ Characteristically for the hydrogen bond system, the charge concentrations on the O–H and N–H covalent bonds are very high. The map of the Laplacian illustrates well-defined charge concentrations on oxygen atoms, indicative of the lone pair existence. The Laplacian distribution at hydrogen atoms involved in hydrogen bonding is very significantly polarized, an effect observed before³⁸ for the hydrogen-bond system. In the case of H(3O), it is polarized exactly towards the O(1) acceptor, while in the case of H(1N) the polarization is in the direction between the two available acceptors. Atomic charges from the monopole populations are illustrated in Fig. 4–6.

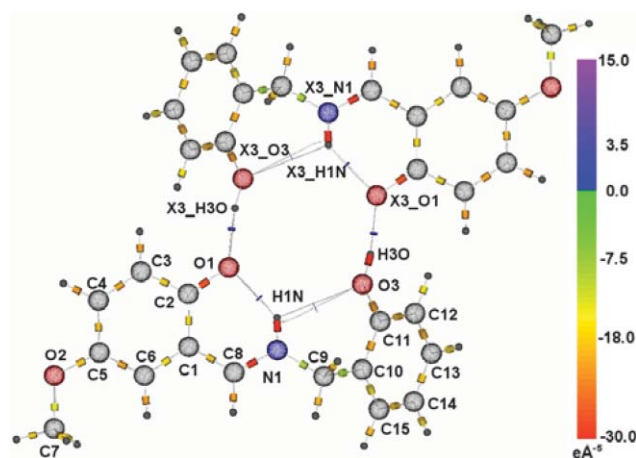


Fig. 4 Molecular graph of the surroundings of the hydrogen-bonding network in the dimer of XV. Labels of atoms from the molecule generated by the X3 symmetry operation are mostly omitted for the sake of clarity. The BCP-s are represented as cylinders. The length of the cylinder is scaled by $\rho(r_{\text{BCP}})$, while its cross-sections illustrate ellipticity at BCP, and colour denotes the value of $\nabla^2\rho(r_{\text{BCP}})$ (violet – positive; green to red – negative). Symmetry operation X3: $1 - x, 2 - y, -z$.

The negative charge is concentrated at all oxygen atoms and also at nitrogen. Carbon atoms do not deviate significantly from neutrality, apart from the methyl group, in which the carbon atom is positively charged. This may be an effect of polarization or a sign of slight rotational disorder of the methyl group. The trends are in general preserved in the case of charges integrated over atomic basins. The oxygen atoms are all significantly negative, as well as the nitrogen atom. The C(7) methyl carbon is significantly positively charged, and so is the C(8) carbon involved in imine bond. There is a significant charge alternation along the bonds enclosing two intermolecular hydrogen bonds: O(1)–C(2)–C(1)–C(8)–N(1)–C(9)–C(10)–C(11)–O(3), while carbon atoms belonging to ring C(1)–C(6) tend to be slightly positive, and those belonging to C(10)–C(15) tend to be slightly negative. Hydrogen atoms involved in H-bonds are both distinguished by significant positive integrated atomic charges, in the case of H(3O) exceeding 0.5 e.

According to Gatti *et al.*,³⁹ the source function allows for a classification of hydrogen bonds in terms of characteristic source contributions to the density at the H-bond critical point from the H involved in the H-bond, the H-donor (D), and the H-acceptor (A).

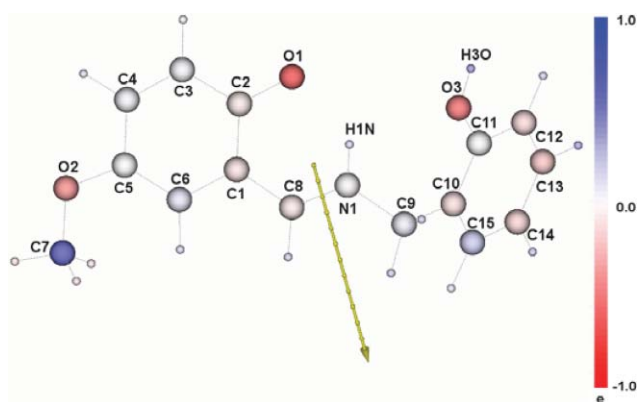


Fig. 5 Atomic charge distribution with numerical values below (AIM atomic charges in bold, and charges resulting from monopole populations). The direction of resulting dipole moment is shown as a yellow arrow. Atomic charges: O(1), -0.53(2), **-1.096**; O(2), -0.34(2), **-1.033**; O(3), -0.43(2), **-1.094**; N(1), -0.01(5), **-0.919**; C(1), -0.08(3), **-0.098**; C(2), -0.06(3), **0.501**; C(3), 0.01(3), **0.015**; C(4), 0.01(3), **0.004**; C(5), -0.01(3), **0.415**; C(6), 0.06(3), **0.060**; C(7), 0.49(4), **0.710**; C(8), -0.06(3), **0.469**; C(9), 0.04(4), **0.316**; C(10), -0.09(3), **-0.104**; C(11), -0.00(3), **0.437**; C(12), -0.10(3), **-0.093**; C(13), -0.17(4), **-0.113**; C(14), -0.13(4), **-0.066**; C(15), 0.14(4), **0.125**; H(3), -0.02(2), **-0.029**; H(4), 0.07(2), **0.061**; H(6), 0.09(2), **0.075**; H(7A), -0.05(1), **-0.021**; H(7B), -0.05(1), **-0.021**; H(7C), -0.05(1), **-0.018**; H(8), 0.10(2), **0.069**; H(9A), 0.13(2), **0.097**; H(9B), 0.12(2), **0.099**; H(12), 0.11(2), **0.091**; H(13), 0.23(2), **0.187**; H(14), 0.13(2), **0.064**; H(15), 0.05(2), **0.044**; H(1N), 0.09(3), **0.301**; H(3O), 0.27(2), **0.505**.

The source contribution from the H appears as the most distinctive marker of the H-bond strength, being highly negative for isolated H-bonds, slightly negative for polarized charge assisted H-bonds, close to zero for resonance-assisted H-bonds, and largely positive for charge-assisted H-bonds. The contributions from atoms other than H, D, and A strongly increase with decreasing H-bond

strength, consistent with the parallel increase in the electrostatic character of the interaction. In terms of such a classification, three hydrogen bonds present in the structure XV are very distinct. The intermolecular, linear O(3)–H(3O)···O(1) hydrogen bond, already classified as the strongest due to geometrical parameters, is a very strong and charge-assisted hydrogen bond in the source function classification, as the H(3O) hydrogen has a positive source contribution, and the combined hydrogen donor, acceptor and H(3O) contributions constitute nearly 90% of all inputs to charge density in this bond. The N(1)–H(1N)···O(1) hydrogen bond is a medium strength hydrogen bond (only about 50% of the source contributions come from atoms belonging to that bond). Interestingly, its characteristics (*i.e.* significantly negative source contribution from the H(1N) hydrogen and the donor contribution being larger than that of acceptor by nearly 10%) suggest that this hydrogen bond is rather polarization- than resonance-assisted.^{39,40} This is counterintuitive to the location of hydrogen bond inside the conjugated system. The third hydrogen bond is extremely weak in terms of source contributions. Only atoms which do not directly constitute this bond, have positive contributions to the charge density at its bond critical point. Source contributions to the critical points of all three hydrogen bonds have been calculated, and are presented in Table 4.

Conclusions

A series of sixteen Schiff bases, which can form different types of intramolecular hydrogen bonds, has been investigated, applying several NMR methods both in the solution and solid state. Additionally, the X-ray structures have been established for three of them. This series of Schiff bases, derivatives of salicylaldehydes and aminophenols or hydroxybenzylamine, consists of four subgroups defined according to presence and position of additional OH

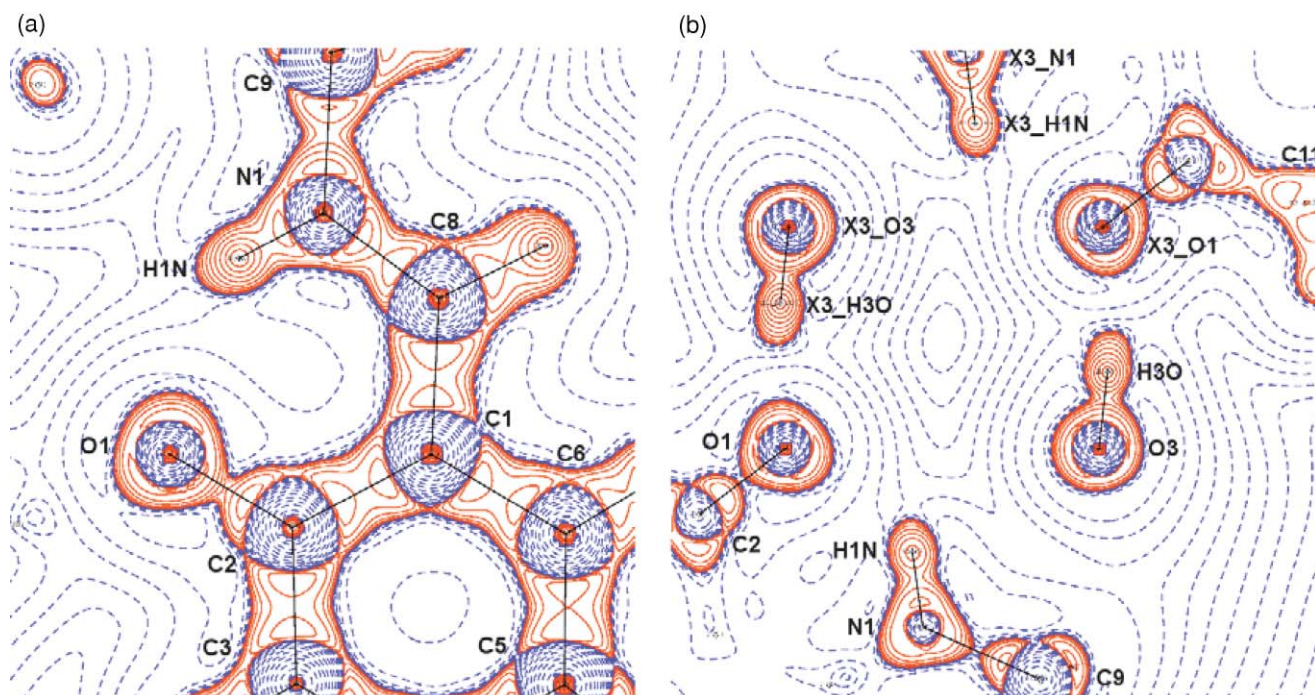


Fig. 6 Laplacian maps of the Schiff base fragment (a) and hydrogen bond network (b).

Table 4 Source function analysis for hydrogen bonds in **XV**. Symmetry operation X3: 1 - x, 2 - y, -z

	D...A [Å]	D-H [Å]	H...A [Å]	$\rho(r_{\text{BCP}})$ [$e \text{ \AA}^{-3}$]	$\nabla^2(r_{\text{BCP}})$ [$e \text{ \AA}^{-5}$]	S_{D} [%]	S_{H} [%]	S_{A} [%]	$S_{\text{D+H+A}}$ [%]
O(1)–H(1N)	2.6016(3)	0.8784(2)	1.8882(3)	0.26(1)	3.33(1)	32.5	-9.9	24.7	47.4
O(1)–X3_H(3O)	2.5332(3)	0.8823(3)	1.6598(2)	0.47(4)	2.33(7)	35.9	9.8	40.0	85.6
O(3)–H(1N)	2.8889(3)	0.8784(2)	2.4492(3)	0.066(5)	1.34(2)	-1.0	-56.2	-48.3	-105.6

group and the length of the linker. Typical hydrogen bonds, involving hydroxyl groups from the parent aldehydes, are formed in all investigated compounds. No 5-membered rings involving the OH-groups in 2' position were found.

The X = H, OCH₃ and halogen-substituted compounds from families **A** and **A'** exist in solution as the OH H-bond form with some asymmetric intramolecular hydrogen bonding, while the 5-nitro compounds exist as the hydrogen-bonded NH. Based on the nitrogen and carbon chemical shifts, it appears that only the OH groups at the position 2 are involved in the hydrogen bond formation (with the O to N proton transfer) in all studied compounds. In the solid state, compounds **XIII–XVI** exist in the NH form with only very small differences at the hydrogen atom positions.

The third group of compounds, **IX–XII** (group **C**) is very similar to group **B**, and can form only one type of H-bonds because they do not have a second hydroxyl group at a suitable position (2'). In the case of the **IX**, **XI** and **XII**, some very similar hydrogen bonds exist in both phases with the hydrogen atom located close to oxygen, as confirmed by the nitrogen chemical shifts of the imine atoms. Again in the 5-nitro derivative **X**, the contribution of the NH form is much higher in solution, and this structure dominates in the solid state.

In the solid state, the contribution of the NH hydrogen bond form in family **B** is generally higher than in family **C**. In DMSO solution the tautomeric equilibrium for 5-nitro derivative **II** is less shifted to the NH form compared to compound **X**. The remaining compounds from this group (**I**, **III** and **IV**) have in DMSO solution very similar structure to **XII**, **XV** and **XVI** respectively.

X-ray structures of the compounds **VII**, **XV** and **XVI** reveal intricate networks of both intra- and intermolecular H-bonds for these compounds. In the case of **VII** (group **A**), the network results in the infinite chain of molecules along the [010] crystallographic direction, whereas compounds **XV** and **XVI** from group **A'** display a common motif, forming dimers bound by intermolecular H-bonds. All three structures proved the existence of strong intermolecular H-bonds, as well as very weak additional intramolecular H-bonds involving the nitrogen and the oxygen from 2'-OH group. These interactions were undetectable by means of carbon and nitrogen chemical shift analysis, because they did not involve proton transfer from 2'-OH hydroxyl group onto the nitrogen atom.

The intramolecular hydrogen bonds in **XV** differ significantly in terms of charge density properties. According to the results from the experimental charge densities, the O(1)···H(1N)–N(1) bond is strong, with significant charge density concentration at the bond critical point, and a straight, well-defined bond path. The same comment is true in the case of the intermolecular O(1)···H(3O)–O(3) bond. In contrast, the second intramolecular hydrogen bond is weak, showing charge density concentration over five times less than the other H-bonds, and a bent bond path. In terms of

energy densities, the weak O(3)···H(1N)–N(1) hydrogen bond is a non-bonding interaction, with total energy density being slightly positive. It can be qualified as pure closed-shell interaction. The strong hydrogen bonds both qualify as shared-shell interactions with respect to $H(r_{\text{BCP}})$ and $G(r_{\text{BCP}})/\rho(r_{\text{BCP}})$.

The intermolecular, linear O(3)–H(3O)···O(1) hydrogen bond has a positive source contribution from the H(3O) hydrogen, and the combined hydrogen donor, acceptor and H(3O) contributions constitute nearly 90% of all inputs to charge density at the BCP of this bond. In the case of the N(1)–H(1N)···O(1) hydrogen bond, only about 50% of the source contributions come from atoms belonging to that bond. A significantly negative source contribution from H(1N) hydrogen, and the donor contribution being larger than that of acceptor by nearly 10%, suggest that this hydrogen bond is polarization- rather than resonance-assisted, which is counterintuitive to the location of hydrogen bond in the conjugated system. In the case of the third hydrogen bond, it is extremely weak in terms of source contributions, and it seems to be an interaction resulting mainly as an effect of the presence of two strong hydrogen bonds in its vicinity.

Acknowledgements

Single-crystal X-ray measurements were carried out at the Structural Research Laboratory of the Chemistry Department, Warsaw University, Poland, established with financial support from the European Regional Development Fund in the Sectoral Operational Programme "Improvement of the Competitiveness of Enterprises, years 2004–2006" project no: WKP_1/1.4.3./1/2004/72/72/165/2005/U. KW thanks financial support from the Ministry of Science and Higher Education – grant 1 T09A 116 30. KW and AM thank financial support from the Foundation for Polish Science "MASTER" professorship.

References

- 1 E. Hadjoudi, *Mol. Eng.*, 1995, **5**, 301 and references cited therein.
- 2 T. Dziembowska, *Pol. J. Chem.*, 1998, **72**, 193 and references cited herein.
- 3 A. Filarowski, *J. Phys. Org. Chem.*, 2005, **18**, 686 and references cited therein.
- 4 W. Schilf and L. Stefaniak, *Bull. Pol. Ac.: Chem.*, 1998, **46**, 15.
- 5 A. Koll, *Int. J. Mol. Sci.*, 2003, **4**, 434.
- 6 W. Schilf, B. Kamiński, T. Dziembowska, Z. Rozwadowski and A. Szady-Chelmieńska, *J. Mol. Struct.*, 2000, **33**, 552.
- 7 A. Szady-Chelmieńska, E. Grech, Z. Rozwadowski, T. Dziembowska, W. Schilf and B. Kamiński, *J. Mol. Struct.*, 2001, **125**, 565–566.
- 8 W. Schilf, B. Kamiński, A. Szady-Chelmieńska and E. Grech, *Solid State Nucl. Magn. Reson.*, 2000, **18**, 97.
- 9 W. Schilf, B. Kamiński and T. Dziembowska, *J. Mol. Struct.*, 2002, **41**, 602–603.
- 10 W. Schilf, B. Kamiński, B. Kołodziej, E. Grech, Z. Rozwadowski and T. Dziembowska, *J. Mol. Struct.*, 2002, **615**, 141.
- 11 T. Dziembowska, K. Ambroziak, Z. Rozwadowski, W. Schilf and B. Kamiński, *Magn. Reson. Chem.*, 2003, **41**, 135.

- 12 G. Wojciechowski, P. Przybylski, W. Schilf, B. Kamiński and B. Brzezinski, *J. Mol. Struct.*, 2003, **649**, 197.
- 13 W. Schilf, B. Kamiński, Z. Rozwadowski, K. Ambroziak, B. Bieg and T. Dziembowska, *J. Mol. Struct.*, 2004, **700**, 61.
- 14 G. Wojciechowski, M. Ratajczak-Sitarz, A. Katrusiak, W. Schilf, P. Przybylski and B. Brzezinski, *J. Mol. Struct.*, 2003, **650**, 191.
- 15 W. Schilf, J. P. Bloxidge, J. R. Jones and S.-Y. Lu, *Magn. Reson. Chem.*, 2004, **42**, 556.
- 16 W. Schilf, *J. Mol. Struct.*, 2004, **689**, 245.
- 17 B. Kołodziej, P. M. Dominiak, A. Kosciółka, W. Schilf, E. Grech and K. Woźniak, *J. Mol. Struct.*, 2004, **691**, 133.
- 18 W. Schilf, B. Kamiński, A. Szady-Chelmieńska and E. Grech, *J. Mol. Struct.*, 2004, **700**, 105.
- 19 Z. Rozwadowski, K. Ambroziak, M. Szypa, E. Jagodzinska, S. Spychaj, W. Schilf and B. Kamiński, *J. Mol. Struct.*, 2005, **734**, 137.
- 20 W. Schilf, B. Kamiński, A. Szady-Chelmieńska and E. Grech, *J. Mol. Struct.*, 2005, **743**, 237.
- 21 Z. Rozwadowski, W. Schilf and B. Kamiński, *Magn. Reson. Chem.*, 2005, **43**, 573.
- 22 V. A. Ozeryanskii, A. F. Pozharskii, W. Schilf, B. Kamiński, W. Sawka-Dobrowolska, L. Sobczyk and E. Grech, *Eur. J. Org. Chem.*, 2006, 782.
- 23 W. Schilf, B. Kołodziej and E. Grech, *J. Mol. Struct.*, 2006, **791**, 93.
- 24 W. Schilf, B. Kamiński, A. Szady-Chelmieńska, E. Grech, A. Makal and K. Woźniak, *J. Mol. Struct.*, 2007, **94**, 844–845.
- 25 B. Kołodziej, E. Grech, W. Schilf, B. Kamiński, M. Makowski, Z. Rozwadowski and T. Dziembowska, *J. Mol. Struct.*, 2007, **32**, 844–845.
- 26 W. Schilf, P. Cmoch, A. Szady-Chelmieńska and E. Grech, *J. Mol. Struct.*, 2009, **921**, 34–37.
- 27 C. C. Ersanli, C. Albayrak, M. Odabasoglu and A. Erdonmez, *Acta Crystallogr., Sect. E: Struct. Rep. Online*, 2004, **60**, o389.
- 28 I. Majerz, A. Pawlukoja, L. Sobczyk, T. Dziembowska, E. Grech and A. Szady-Chelmieńska, *J. Mol. Struct.*, 2000, **552**, 243.
- 29 T. M. Krygowski, K. Woźniak, R. Anulewicz, D. Pawlak, W. Kołodziej, E. Grech and A. Szady, *J. Phys. Chem.*, 1997, **101**, 9399.
- 30 K. Pyta, P. Przybylski, W. Schilf, B. Kołodziej, E. Grech, A. Szady-Chelmieńska and B. Brzezinski, *J. Mol. Struct.*, 2010, **967**(1–3), 140–146.
- 31 H. Pizzala, M. Carles, W. E. E. Stone and A. Thevand, *J. Chem. Soc., Perkin Trans. 2*, 2000, 935.
- 32 N. Galic, Z. Cimerman and V. Tomisic, *Anal. Chim. Acta*, 1997, **343**, 135.
- 33 M. C. Etter, J. C. MacDonald and J. Bernstein, *Acta Crystallogr., Sect. B: Struct. Sci.*, 1990, **46**, 256–262.
- 34 P. M. Dominiak, E. Grech, G. Barr, S. Teat, P. R. Mallinson and K. Woźniak, *Chem.–Eur. J.*, 2003, **9**(4), 963–970.
- 35 U. Koch and P. L. A. Popelier, *J. Phys. Chem.*, 1995, **99**, 9747.
- 36 P. A. Wood, F. H. Allen and E. Pidcock, *CrystEngComm*, 2009, **11**, 1563.
- 37 P. M. Dominiak, A. Makal, P. R. Mallinson, K. Trzcinska, J. Eilmes, E. Grech, M. Chruszcz, W. Minor and K. Woźniak, *Chem.–Eur. J.*, 2006, **12**(7), 1941–1949.
- 38 J. Overgaard, B. Schiøtt, F. K. Larsen and B. B. Iversen, *Chem.–Eur. J.*, 2001, **7**, 3756.
- 39 C. Gatti, F. Cargnoni and L. Bertini, *J. Comput. Chem.*, 2003, **24**, 422–436.
- 40 G. Gilli and P. Gilli, *J. Mol. Struct.*, 2000, **552**(1–3), 1–15.